Journal of Alloys and Compounds 553 (2013) 35–39

Contents lists available at SciVerse ScienceDirect

Journal of Alloys and Compounds

journal homepage: www.elsevier.com/locate/jalcom

Nanocrystal formation using laser irradiation on Nd^{3+} doped barium titanium silicate glasses

L.L. Martin [a,*], S. Ríos [b], I.R. Martín [a,c], P. Haro-González [a], J.M. Cáceres [d], A. Hernández-Creus [e]

[a] Dpto. Física Fundamental y Experimental, Electrónica y Sistemas, Instituto de Materiales y Nanotecnología, Universidad de La Laguna, Av. Astrofísico Francisco Sánchez, s/n, E-38206 La Laguna, Tenerife, Spain
[b] Dpto. de Física Básica, Universidad de La Laguna, Av. Astrofísico Francisco Sánchez, s/n, E-38206 La Laguna, Tenerife, Spain
[c] MALTA Consolider Team, Spain
[d] Dpto. Edafología y geología, Universidad de La Laguna, Av. Astrofísico Francisco Sánchez, s/n, E-38206 La Laguna, Tenerife, Spain
[e] Dpto. de Química Física, Instituto de Materiales y Nanotecnología, Universidad de La Laguna, Av. Astrofísico Francisco Sánchez, s/n, E-38207 La Laguna, Tenerife, Spain

ARTICLE INFO

Article history:
Received 29 June 2012
Received in revised form 12 September 2012
Accepted 28 October 2012
Available online 6 November 2012

Keywords:
Nd^{3+}
Laser irradiation
$Ba_2TiSi_2O_8$
Nanocrystals
Glass ceramic
Glass

ABSTRACT

Two different thermal treatments were used to create nanocrystals from a precursor glass. The glass whose composition is $Ba_2TiSi_2O_8$ and doped with 3% of Nd^{3+} was prepared using the melt quenching method. A conventional thermal treatment in an electrical furnace was used to obtain transparent glass ceramic samples, which contain Fresnoite nanocrystals with an average size of 35 nm. Moreover, these nanocrystals were obtained in a localized area of the precursor glass by irradiating with a continuous Ar^+ laser. Evidence of the changes induced by laser irradiation was confirmed by optical spectroscopic, X-ray diffraction, scanning electron and atomic force microscopy.

1. Introduction

The glass–ceramic materials are produced by a controlled devitrification or crystallization from a precursor glass. This process differs from the spontaneous crystallization that is a common problem in the glass production. After the devitrification process, the glass–ceramic material contains an amorphous phase of the remaining glass and one or more nanocrystalline phases, all resulting in a mixture of properties.

Transparent glass–ceramics containing rare-earth ions or nonlinear optical crystals have received considerable attention, because such materials have high potential applications in photonics [1,2]. From the viewpoint of practical applications in integrated optics or photonic crystals, it is important to fabricate transparent glass–ceramics with controlled patterns as micro-scale dots or lines, which can be used as laser waveguides, gratings or wavelength conversion devices. Laser irradiation of glass materials has recently been successfully used as an effective technique to induce spatially selected structural modification and/or crystallization in glass [3,4]. This technique is of particular interest for performing various optical devices to form crystalline phases in glass through this laser irradiation.

Fresnoite crystal, composed of barium–titanium silicate $Ba_2TiSi_2O_8$ (BTS), belonging to P4bm group, has TiO_5 square pyramidal structure, which is the origin of the polarizability of this crystal [5]. BTS crystal shows piezoelectric, pyroelectric, ferroelectric, fluorescence and non-linear optical properties [6,7]. Recently Maruyama et al. [8] reported the possibility of synthesizing transparent glass ceramic samples by heat treatment of glasses using an electric furnace. These transparent nanocrystalline materials have important applications in photonic devices where complex structures of small size, only obtained by laser irradiation, are required. Also, the possibility of fabricate high quality optical micro-resonators made from BTS glass have been shown [9] and the capability of modifying these structures is only possible by micro structuring with laser devitrification.

The aim of this work is to analyze the changes produced in Nd^{3+} doped BTS precursor glass under irradiation with continuous wave Ar^+ laser. In this work the effect of laser irradiation on glass samples is compared to the behavior of glass ceramic samples obtained by thermal treatment in order to determine the optimal conditions to produce nanocrystalline material upon laser exposure.

* Corresponding author. Tel.: +34 922 318 651.
E-mail address: lmartin@ull.es (L.L. Martin).
URL: http://lmartin.webs.ull.es/ (L.L. Martin).

0925-8388/$ - see front matter © 2012 Elsevier B.V. All rights reserved.
http://dx.doi.org/10.1016/j.jallcom.2012.10.162

2. Experimental

A glass with a composition of $40BaO–20TiO_2–40SiO_2$ and doped in excess by 1.5 Nd_2O_3 (in mol%) was prepared using a conventional melt-quenching method. Commercial powders of reagent grade $BaCO_3$, TiO_2, SiO_2 and Nd_2O_3 were mixed and melted in a platinum–rhodium crucible at 1500 °C for 1 h in an electric furnace. After that, the melt was poured between two bronze plates at 200 °C. The samples were then annealed at 650 °C and cooled down slowly to room temperature for 24 h. The samples were polished to obtain a smooth and flat surface in both faces, in order to ensure that the laser does not diverge when irradiates the sample.

The glass ceramic samples were obtained by thermal treatment of the precursor glass at 860, 840 and 820 °C for 20 min, being the sample obtained at 820 °C the most transparent one while still showing the characteristics of a glass ceramic. These samples were used as a pattern to compare the luminescence and X-ray diffraction (XRD) with that showed by the glass exposed to laser irradiation.

In the laser irradiation experiment, a multiline continuous Ar^+ laser was focused on the surface of the glass sample, increasing the laser power up to 3.8 W. This laser beam has a Gaussian profile with a full width at half maximum of 1.4 mm. It was focalized on the sample using a 20 mm focal lens. The diameter of the focalized spot d_1 at $1/e^2$ of the intensity peak is given by the formula:

$$d_1 = \frac{\lambda f}{\pi d_2} \quad (1)$$

where λ is the excitation wavelength, f the focal length of the lens and d_2 the diameter of the collimated pumping beam before the lens. A mean diameter of about 23 μm is obtained for the pump spot on the sample. Therefore, at the maximum laser power in this experiment (about 3.8 W) the corresponding power density is about 250 kW/cm^2.

To characterize the samples a confocal micro-luminescence microscope has been used. The optical setup has been described in detail in a previous work [10]. The sample is located at the focal plane of a 20× microscope objective on a motorized translation stage and excited using a c.w. DPSS laser at 532 nm. The luminescence is detected using a CCD spectrograph. Optical emission spectra were recorded in regions inside and outside the laser irradiated area. Luminescence measurements were averaged in a prolate ellipsoid of about 1.35 μm^3. It is important to remark the need of keeping this volume small enough to avoid contributions from the bulk glass under the superficial modification.

X-ray diffraction measurements have been also obtained for the different samples (glass, glass ceramic and irradiated area) using a Panalytical X'Pert diffractometer for poly-crystalline samples, allowing a direct and comprehensible corroboration of the amorphous and nanocrystalline phases in the studied samples.

To study the morphology of the irradiated area of the sample some complementary measurements were carried out. Atomic Force Microscope (AFM) and Scanning Electron Microscope (SEM) were used to image the surface of the sample and Energy Dispersive X-ray spectroscopy (EDX) to confirm that the properties of the glass irradiated area corresponds to Fresnoite nanocrystals. The surface topography made with the atomic force microscope (AFM) was carried out operating in tapping mode (Nanoscope V from Digital Instrument/Bruker) in air at room temperature. Etched silicon tips RTESP, 215–254 kHz, 20–80 N/m were used.

3. Results and discussion

The XRD measurements have been performed on the bulk glass ceramic, bulk precursor glass and irradiated area. In Fig 1, the black line corresponds to the XRD pattern of glass sample, where a broad diffraction curve without significant structure is clearly observed, as expected for an amorphous material. The red curve represents the XRD of the glass ceramic sample produced at 820 °C, showing the characteristic narrow peaks associated to the presence of nanocrystals. All XRD peaks are assigned to the so-called Fresnoite $Ba_2TiSi_2O_8$ crystalline phase (space group P4bm, JCPDS: No. 022-0513), indicating that the devitrification process is controlled and leads to the formation of only Fresnoite crystals (the theoretical peaks for this phase is also included in Fig. 1). The average size of the precipitated BTS nanocrystals has been estimated to be around 35 ± 5 nm using the Scherrer formula [11].

Fig. 2 shows a SEM image of the irradiated area in the glass sample. The central hole produced by laser ablation is surrounded by an almost circular area corresponding to the modified region of the glass sample. This area extends radially up to 600 μm and has lack of symmetry in the left side due to the differences in thermal conductivity in the vicinity of the sample boundaries (the heat flow is larger toward the center of the sample than towards the air-sample interface direction because the lower thermal conductivity of the air). It is interesting to note that the focused laser spot is about 23 μm and the modified zone is wider. The thermal conductivity of the material is the responsible of the increase of the affected zone due to the thermal effects. The XRD measurement of this irradiated area is included in Fig. 1. It can be seen that the peaks in the XRD are in good agreement with the theoretical ones, confirming that the devitrification obtained by continuous laser heating leads to Fresnoite nanocrystals formation. The estimated size of these nanocrystals is 35 ± 15 nm, where the increase in uncertainly respect to the values obtained under furnace treatment comes from the lower signal to noise ratio (SNR) on the data. This decrease of the SNR is due to a reduction of intensity in the irradiated area and the use of a small region of the sample to avoid the inclusion of the non-irradiated area in the XRD measurements. A detailed comparison of the XRD from the glass ceramic samples produced using a furnace at 820 °C

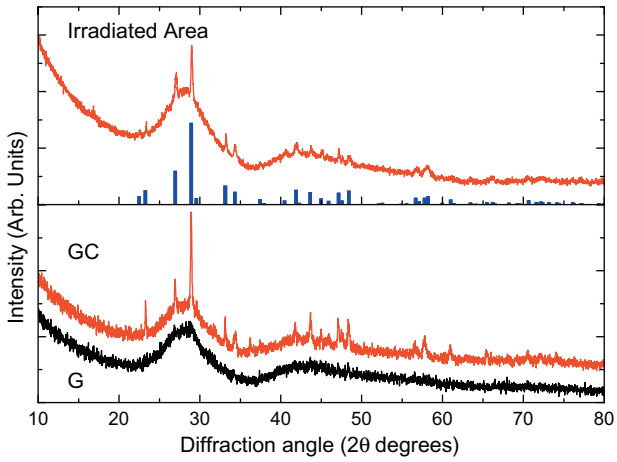

Fig. 1. X-ray diffraction patterns of samples showing the presence of Fresnoite nanocrystals. XRD patterns of a bulk glass (G), a glass–ceramic (GC) and the irradiated area. The theoretical diffraction peak positions for a Fresnoite crystal (blue) are also included. (For interpretation of the references to color in this figure legend, the reader is referred to the web version of this article.)

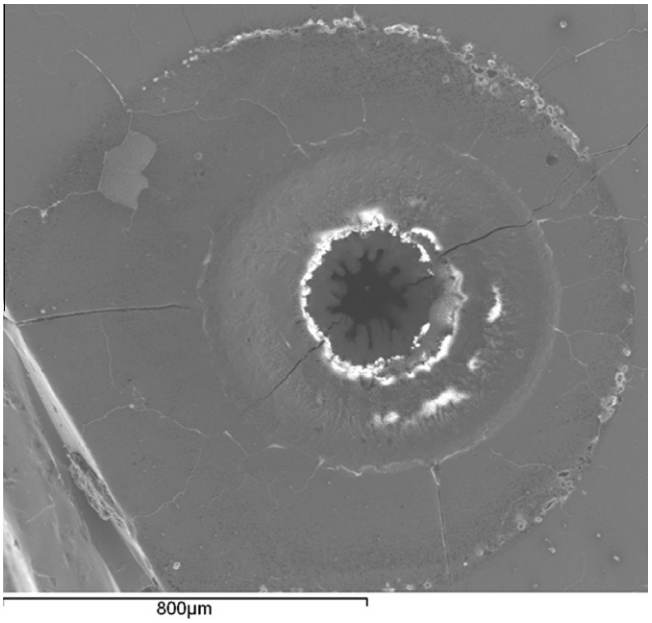

Fig. 2. Scanning electron microscope image of the irradiated area.

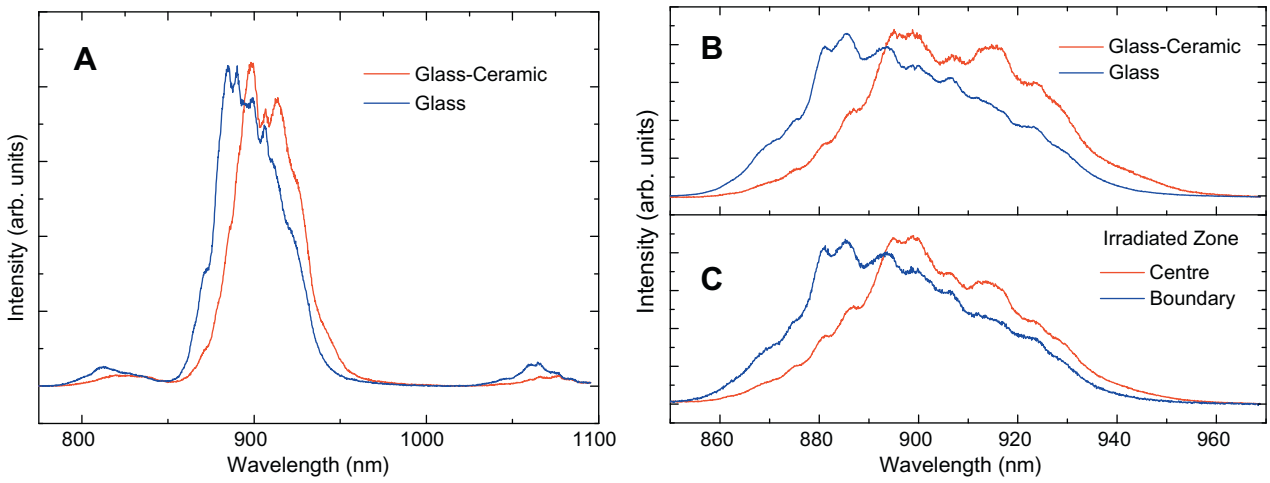

Fig. 3. Normalized spectra of bulk glass and glass ceramic samples, produced by thermal treatment (A). Emission bands corresponding to Nd^{3+}:$^4F_{3/2} \rightarrow {}^4I_{11/2}$ transition of bulk glass and glass ceramic samples obtained by thermal treatment (B). The same transition in the center and in the boundary of the irradiated area, showing glass ceramic formation in the central region due to laser heating (C). (For interpretation of the references to color in this figure legend, the reader is referred to the web version of this article.)

and those obtained at 840 and 860 °C does not show any significant variation in the nanocrystal sizes with the temperature.

Luminescence spectra have been obtained on the precursor glass and on the glass ceramic samples, as shown in Fig. 3A. These spectra were recorded in the range of 600–1100 nm under laser excitation at 532 nm and normalized for a better comparison. Three emission bands associated to the f–f transitions Nd^{3+}:$^4F_{5/2} \rightarrow {}^4I_{9/2}$ (820 nm), $^4F_{3/2} \rightarrow {}^4I_{9/2}$ (890 nm) and $^4F_{3/2} \rightarrow {}^4I_{11/2}$ (1060 nm) are observed. There are some significant differences in the shape of these emissions between the precursor glass and the glass ceramic samples, being especially remarkable the $^4F_{3/2} \rightarrow {}^4I_{9/2}$ (890 nm) emission band whose signal dominates in these measurements. Fig. 3B shows an extended view of the $^4F_{3/2} \rightarrow {}^4I_{9/2}$ transition where these differences can be easily observed for the bulk glass and glass ceramic samples. The principal difference between the glass and glass–ceramic luminescence is the red-shift about 20 nm produced in the glass ceramic respect to the glass. This result makes that the $^4F_{3/2} \rightarrow {}^4I_{9/2}$ transition is an excellent indicator to determine if the studied sample is glass or glass ceramic. Hence, the relation of intensities at 915 and 886 nm is about 2 for the glass ceramics and 0.5 for the glass, making easy to determine if a given spectra corresponds to a glass or to a glass–ceramic phase. This transition is also shown in Fig. 3C for the irradiated area. The values of the intensity ratio in the boundary and center of the irradiated zone show that this regions behave as glass ceramic and glass, respectively. In order to analyze these changes more carefully, individual spectra in this region have been obtained and a mapping showing the ratio of intensities at 915 and 866 nm for the $^4F_{3/2} \rightarrow {}^4I_{9/2}$ transition has been shown in Fig. 4. It can be seen that the devitrified area extends radially from the central hole at about 400 μm and that a thin ring of bulk glass with a radius of 150 μm appears surrounding the central hole. This behavior is based on the ablation process, where a fraction of the material in the center of the focused spot is shifted faraway of this zone, forming a ring with an amorphous behavior.

Fig. 5 shows four EDX mappings superimposed to the SEM image, where the intensity is proportional to the relative content of the selected element, corresponding to the main elements present in the sample: Ba, Ti, Si and O. The Nd was not considered because the low absolute content (only 3% in the precursor glass). On all the images the relative content does not change meaningfully in contrast to other studies in a different matrix [4]. The main reason is that the composition of the glass is nearly stoichiometric equal

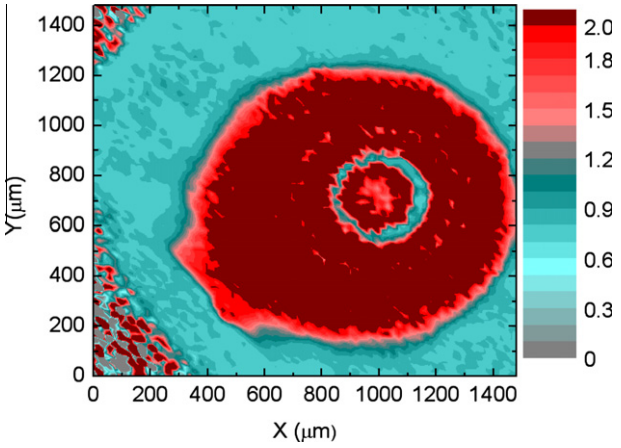

Fig. 4. Image constructed from a spectral mapping where each point corresponds to the relation of intensities at and 886 nm. According to the color bar, the red colored area corresponds to a glass–ceramic zone and the blue to the glass. (For interpretation of the references to colour in this figure legend, the reader is referred to the web version of this article.)

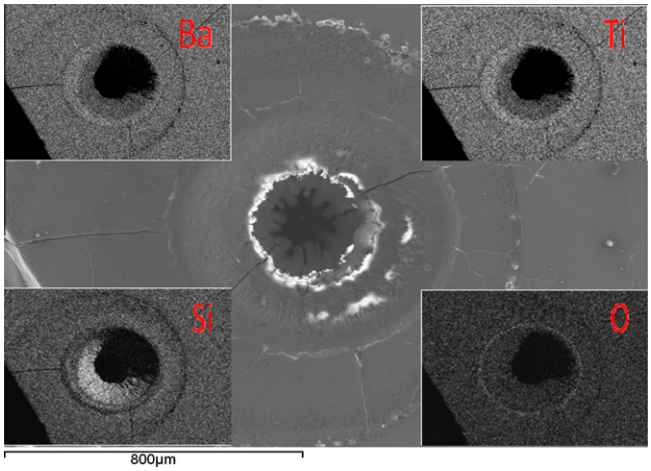

Fig. 5. Energy-dispersive X-ray spectroscopy image, showing the relative content for barium, titanium, oxygen and silicon. Superimposed to the SEM image.

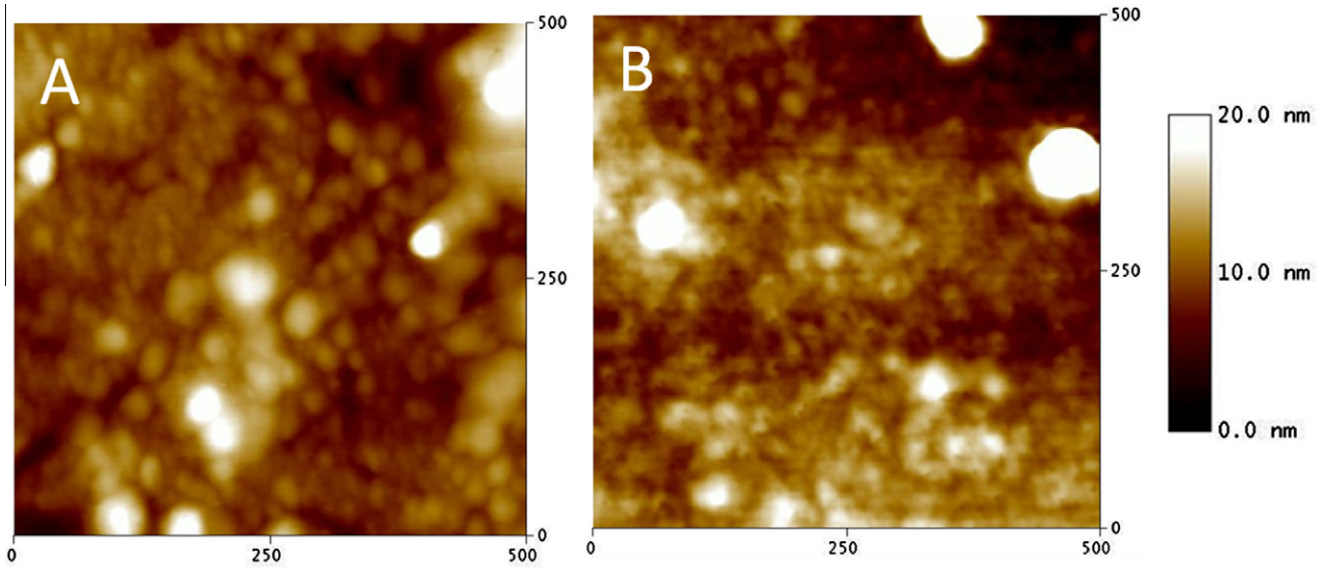

Fig. 6. AFM (500 nm × 500 nm) images corresponding to the glass sample in the non-irradiated (A) and irradiated zones (B).

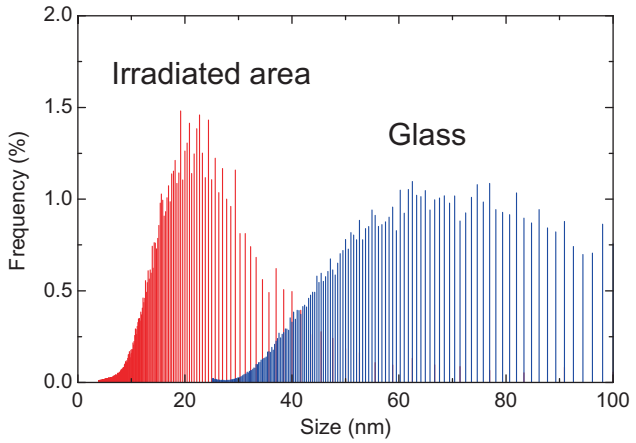

Fig. 7. Size distribution of the particles obtained from the Figs. 6A and B corresponding to the non-irradiated (precursor glass) and irradiated zones, respectively.

to the Fresnoite nanocrystals that are formed inside. There is still a change in intensity on the EDX images not related to the SEM image, due to the different angle of illumination employed, from top on the SEM and at a small angle on EDX. However, the flat and well illuminated areas can be compared and they indicate a similar distribution of main elements present in the sample. The changes that can be observed show agreement with Fig. 4.

Fig. 6A represents the AFM image of a region of the sample where no heating treatment was applied. As can be seen, the surface contains particles of very different sizes, most of them ranging around 80 nm and forming large randomly distributed agglomerates. The roughness of the image is about 5.0 nm. Fig. 6B corresponds to the AFM image of the same sample in the irradiated area where the heating treatment promoted the growth of nanocrystals. Although this figure looks similar to the previous one, the surface roughness has decreased to a value of 2.9 nm. The size of the particles seen in Figs. 6A and B was measured by applying a highpass filter to both the topographic image and the so called contrast phase mode image (not shown). This is the best way to obtain sizes by AFM when, as it is the case, the particles are greater than the tip radius. After the application of a highpass filter, the borders of the particles resulted enhanced without any distorsion in their sizes. Most of the particles are 25–30 nm wide as it is shown in the size distribution in Fig. 7. This result is in good agreement with the average size of 35 ± 15 nm that was obtained from the XRD measurement for the Fresnoite nanocrystals.

4. Conclusions

Localized modifications in BTS precursor glass doped with Nd^{3+} have been induced by laser irradiation. The precursor glass used in this study (doped with 3 mol% of Nd^{3+}) was fabricated by the melt quenching method. BTS glass ceramic samples containing nanocrystals with an average size of 35 nm were obtained by a thermal treatment of this precursor glass. The results obtained from the BTS glass ceramic sample were utilized to compare with those from the irradiated area.

Localized regions of the precursor glass were irradiated by continuous Ar^{+} laser. Evidence of the presence of changes induced by laser exposure was demonstrated by comparing with the spectroscopic properties and XRD patterns of the irradiated regions with those corresponding to the precursor glass and the glass ceramic samples. Moreover, atomic microscope force images confirm the formation of nanocrystals with a similar size in this zone. Confocal micro-luminescent measurements of the emission spectra corresponding to the Nd^{3+} transitions were obtained under laser excitation at 532 nm. The results are consistent with the formation of a crystalline phase as a consequence of continuous laser exposure. Therefore, it is possible to induce the formation of Fresnoite nanocrystals doped with Nd^{3+}, but it is important to control the laser power irradiation in order to avoid ablation process in the sample.

Acknowledgments

Authors thank Ministerio de Economía y Competitividad of Spain (MINECO) within The National Program of Materials (MAT2010-21270-C04-02/-03/-04), The Consolider-Ingenio 2010 Program (MALTA CSD2007-0045, www.malta-consolider.com), the EU-FEDER for their finantial support and ACIISI of Gobierno de Canarias for the project ID20100152 and FPI. We also thank The Governments of Spain and India for the award of a project within the Indo-Spanish Joint Programme of Cooperation in Sci-

ence and Technology (PRI-PIBIN-2011-1153/DST-INT-Spain-P-38-11).

References

[1] Y.H. Wang, J. Ohwaki, Appl. Phys. Lett. 63 (1993) 3268–3270.
[2] Y. Takahashi, Y. Benino, T. Fujiwara, T. Komatsu, J. Non-Cryst. Solids 316 (2003) 320–330.
[3] L.L. Martin, P. Haro-Gonzalez, I.R. Martin, D. Puerto, J. Solis, J.M. Caceres, N.E. Capuj, Opt. Mater. 33 (2010) 186–190.
[4] P. Haro-Gonzalez, I.R. Martin, A. Hernandez Creus, Opt. Express 18 (2010) 582–590.
[5] P.B. Moore, J. Louisnat, Science 156 (1967) 1361–1362.
[6] N. Toyohara, Y. Benino, T. Fujiwara, T. Komatsu, Solid State Commun. 140 (2006) 299–303.
[7] H. Masai, S. Tsuji, T. Fujiwara, Y. Benino, T. Komatsu, J. Non-Cryst. Solids 353 (2007) 2258–2262.
[8] N. Maruyama, T. Honma, T. Komatsu, J. Solid State Chem. 182 (2009) 246–252.
[9] L.L. Martin, C. Perez-Rodriguez, P. Haro-Gonzalez, I.R. Martin, Opt. Express 19 (2011) 25792–25798.
[10] L.L. Martin, P. Haro-Gonzalez, I.R. Martin, D. Navarro-Urrios, D. Alonso, C. Perez-Rodriguez, D. Jaque, N.E. Capuj, Opt. Lett. 36 (2011) 615–617.
[11] S. Schiller, Appl. Opt. 32 (1993) 2181–2185.